LAWRENCE
LIVERMORE
NATIONAL
LABORATORY

UCRL-JRNL-236499

Demonstrating fractal scaling of residence time distributions on the catchment scale using a fully-coupled, variably-saturated groundwater and land surface model and a Lagrangian particle tracking approach

S. J. Kollet, R. M. Maxwell

November 13, 2007

Geophysical Research Letters

Disclaimer

Demonstrating fractal scaling of residence time distributions on the catchment scale using a fully-coupled, variably-saturated groundwater and land surface model and a Lagrangian particle tracking approach

Stefan J. Kollet[1, 2] and Reed M. Maxwell[2]

Atmospheric, Energy, and Environmental Sciences Division

Lawrence Livermore National Laboratory

ABSTRACT - The influence of the vadose zone, land surface processes, and macrodispersion on scaling behavior of residence time distributions (RTDs) is studied using a fully coupled watershed model in conjunction with a Lagrangian, particle-tracking approach. Numerical experiments are used to simulate groundwater flow paths from recharge locations along the hillslope to the streambed. These experiments are designed to isolate the influences of topography, vadose zone/land surface processes, and macrodispersion on subsurface RTDs of tagged parcels of water. The results of these simulations agree with previous observations that RTDs exhibit fractal behavior, which can be identified from the power spectra. For cases incorporating residence times that are influenced by vadose zone/land surface processes, increasing macrodispersion increases the slope of the power spectra. In general the opposite effect is demonstrated if the vadose zone/land surface processes are neglected. The concept of the spectral slope being a measure of stationarity is raised and discussed.

Introduction

The observation by Kirchner et al. [2000] that long-term time series of stream chemistry exhibit fractal behavior has prompted increased interest in residence time distributions of groundwater from the streambed scale (10^0m) to the continental scale (10^6m) [e.g., *Worman et al.*, 2007]. The main focus of previous work has been on the role of

[1] Current address: Meteorological Institute, Bonn University, Bonn, Germany, stefan.kollet@uni-bonn.de
[2] Authors share equal co-authorship

26 subsurface heterogeneity in solute transport [*Haggerty et al.*, 2000; *LaBolle et al.*, 2006;
27 *Maxwell et al.*, 2003; *Tompson et al.*, 1999], the patterns of vegetation [*Scanlon et al.*, 2007]
28 and the influence of the topography of the upper boundary [*Cardenas*, 2007; *Haggerty et al.*,
29 2002; *Kirchner et al.*, 2001; *Worman et al.*, 2007]. All of these processes are shown to be
30 scale dependent, for example the influence of a topographical upper boundary to groundwater
31 flow may range in scale from streambed ripples to the land surface up to the continental scale.
32 The work presented here, uses a fully-integrated, numerical watershed model that incorporates
33 aspects of all these systems demonstrates scale dependence and points to the relative
34 importance of these various component processes.

35 For the case of steady state conditions and based on the assumption that the water table
36 closely follows the topography of the upper boundary, one can show that topography induces
37 groundwater flow with power law or fractal behavior even if the subsurface is homogeneous.
38 This stems from the presence of stagnation points in the domain, i.e. locations where the flow
39 velocities are zero. These stagnation points generate velocity distributions over a wide range
40 of scales that lead to a wide range in residence time distributions of groundwater [*Cardenas*,
41 2007]. In addition, subsurface heterogeneity can enhance power lower behavior of residence
42 time distributions by additionally producing a range of groundwater velocities and thus
43 residence time distributions [*Haggerty et al.*, 2000]. The self-similarity of groundwater
44 systems has also been observed by many authors (e.g. [*Worman et al.*, 2007]). In a purely
45 hydraulic sense, this self-similarity is evident from an examination of the classical Toth
46 solution [*Toth*, 1963]. Expressed in non-dimensional variables, the solution is valid on all
47 spatial scales as long as Darcy flow is guaranteed. Therefore, one can "zoom" in and out of
48 the potential solution from the streambed scale to the continental scale without changing the
49 basic mechanisms, which is one of the central requirements of self-similarity.

50 The aforementioned studies are based on a suite of assumptions such has steady state
51 conditions of the potential field and that processes of the vadose zone and at the land surface

52 do not exert any influence on subsurface flow, i.e. only flow in the saturated zone is
53 considered. However, even if there is a free water table that closely follows the topography, it
54 may be dynamic due to diurnal and seasonal variations in atmospheric forcing and vegetation.
55 In this case, a steady state solution of the potential field does not suffice. Thus, in order to
56 examine the influence of the land surface and the shallow subsurface on the residence time
57 distributions of groundwater, one requires a more advanced analysis that takes into account
58 the pertinent physical processes, such as three-dimensional variably saturated groundwater
59 flow, root water uptake by plants, evaporation, from the bare soil, infiltration, and overland
60 flow. This has been discussed previously by *Reed et al.*, [2006], who pointed to the need for
61 field measurements on the watershed scale and the development of simulation tools treating
62 the subsurface-land surface-atmosphere system in an integrated fashion.
63 In this study, a novel watershed simulation platform is applied to a catchment with an
64 area on the order of $10^3 km^2$. The simulation platform consists of a parallel, three-dimensional,
65 variably saturated groundwater/surface water flow code, coupled to a land surface model. This
66 fully-coupled model accounts for pertinent processes at, across and below the land surface and
67 is forced by an atmospheric time series, thus, relaxing many of the assumption made in
68 previous studies. Transient particle tracking of a conservative tracer is used to derive
69 residence time distributions of parcels of water recharged either at the water table or at the
70 land surface (thus being influenced by vadose and root zone processes) for a range of
71 macrodispersion. In the ensuing analysis, the power spectra of the distributions of residence
72 time and their slope are computed. The different slopes of the power spectra are related to the
73 simulated processes and to the statistical concept of stationarity.
74
75 **Methods**
76 In order to arrive at residence time distributions that were used in the spectral analysis,
77 a two-step numerical experiment was performed. First, an integrated watershed simulation

platform was applied to a watershed in central Oklahoma (USA), which resulted in a time series of three-dimensional pressure fields in the subsurface. Second, a Lagrangian, particle-tracking method was applied in conjunction with these transient pressure results to develop residence time distributions of subsurface water for the ensuing spectral analysis. Both steps are outlined in more detail below.

Integrated Watershed Simulations

The pressure fields for the particle tracking experiment were obtained from simulations using an integrated watershed numerical code. The methodology and simulation are described in detail in *Kollet and Maxwell* [2007]. The numerical code consists of ParFlow, a parallel, three-dimensional variably saturated groundwater/surface water flow code with an integrated land surface model. The land surface model is the Common Land Model (CLM, [*Dai et al.*, 2003]) and calculates the mass and energy balance at the land surface. ParFlow calculates the moisture redistribution in the shallow subsurface that is influenced by evapotranspiration and infiltration as well as deep groundwater flow. For technical details we refer the reader to [*Ashby and Falgout*, 1996; *Jones and Woodward*, 2001; *Kollet and Maxwell*, 2006; *Kollet and Maxwell*, 2007; *Maxwell and Miller*, 2005].

As described in detail in *Kollet and Maxwell* [2007] the simulation platform was applied to the Little Washita watershed, Oklahoma, USA for the water-year 1999. This model of the Little Washita watershed consisted of a deep, homogeneous aquifer ($\sim 10^2$m), topography, spatially distributed land and soil cover, and overland flow parameters. A one year time series of spatially uniform atmospheric forcing was applied from September 1998 until August 1999 in spinup mode until a dynamic equilibrium was obtained. The spinup procedure resulted in the development of the Little Washita River in the model domain that is the locus of particle injection in the particle tracking experiment.

104 *Residence Time distributions and Spectral Analysis*

105 A Lagrangian, particle-tracking approach, described in detail in previous work
106 [*Maxwell and Kastenberg*, 1999; *Maxwell et al.*, 2003; *Maxwell and Tompson*, 2006; *Maxwell*
107 *et al.*, 2007; *Tompson et al.*, 1998], was used to simulate the evolution of age of tagged
108 parcels of water. Particle-tracking methods have been widely applied in subsurface transport
109 problems [e.g., *LaBolle et al.*, 1996; *Tompson and Gelhar*, 1990]. This particular particle
110 model has been previously applied to simulate water age and to interpret isotopic observations
111 [e.g., *Maxwell et al.*, 2003; *Tompson et al.*, 1999]. Lagragian methods are advantageous in
112 that they allow for rapid simulation of transport and do not suffer from numerical dispersion,
113 making them well-suited for representing accurately transport with very large Peclet numbers.
114 For this simulation, particles placed at the bottom of fully saturated riverbed cells,
115 located within the primary watershed, at a density of 5,000 particles per grid cell for a total
116 number of particles, Np=765,000. Pressure fields advanced daily for 500 years for a total of
117 182,500 timesteps, i.e. the pressure field time series from the one year spinup was averaged
118 daily and repeated 500 times. As in *Tompson et al.,* [1999] and *Maxwell et al.*, [2003], cell
119 velocities are reversed and particles are transported backwards to the source location. All
120 pressure fields are taken from the results of *Kollet and Maxwell* [2007] as mentioned above.
121 For the water table cases (case WT), to mimic an isotopic tracer such as ^{3}H that will re-
122 equilibrate when exposed to the atmosphere, particles were stopped when the saturation
123 dropped below 0.95 and their travel time were recorded. For the vadose zone cases (case LS)
124 particles were not stopped until they reached the land surface. Macrodispersion was added to
125 these transport simulations to represent the dispersive effect of subsurface heterogeneity on
126 transport. While a very approximate representation, this approach allowed for varying the
127 Peclet number,*Pe*, ($\sim L/\alpha_l$) by varying the longitudinal dispersivity over four orders of
128 magnitude and using a hillslope scale of L = 7.5km from *Kollet and Maxwell* [2007] (Table

1). For all simulations the transverse dispersivity was set to $\alpha_l/10$. An example of the spatial distribution of travel time generated using this approach may be seen in Figure 1.

The time distributions created by these reverse particle traces were then binned into one-day increments to create a probability distribution function (PDF) of travel times from any recharge point to the riverbed. Due to the discrete nature of particle tracking, some of the PDF bins contained zero values which were omitted creating an unevenly sampled distribution. These PDF's where then transformed into the spectral domain using the so-called Lomb-Scargle technique for uneven data [*Lomb*, 1976; *Scargle*, 1982] as implemented by *Press et al.,* [1996]. The resultant spectral power-wavelength plots are shown in Figures 2 and 3.

Table 1. Parameter summary for the 8 simulated transport cases.

Case	*Pe*	α_l (m)
WT	75000	0.1
	7500	1
	750	10
	75	100
LS	75000	0.1
	7500	1
	750	10
	75	100

Results and Discussion

Figures 2 and 3 show the power spectra of the residence time distributions calculated from particle path simulations ending at the water table, case WT, and at the land surface, case LS. In all simulations the spectra exhibit power law behavior and fractal scaling that has been observed previously in experimental and theoretical studies [e.g., *Kirchner et al.*, 2000]. Increases in macrodispersion (i.e. a decrease in *Pe* due to an increase in longitudinal dispersivity) act as a low-pass filter and smooth the curves similar to the moving average that is also shown in Figures 2 and 3. Since, the analysis is based on a pressure distribution time series repeating one year of spinup 500 times resulting in a total simulation time of 500 years, the correlation length of the residence time distribution appears to be one year.

In case WT (Figure 2), the slopes of the power spectra, *m*, first increase with increasing heterogeneity and then decrease and range between $0.87<m>1.16$. This dependence of *m* on *Pe* is also illustrated in Figure 4. The range *m* corresponds well with reported values in the literature from experimental and theoretical studies. For example, *Kirchner et al.*, [2000] obtained similar values from the analysis of chloride concentrations from small catchments ($\sim 10^0 km^2$) at the Welsh coast line and nine other catchments spanning a variety of climate and hydrologic conditions. In theoretical studies, *Kirchner et al.*, [2001] only obtained model results that produced fractal scaling by using very large macrodispersivities, i.e. $Pe \leq 1$. Thus, the range of *m* obtained from the measured data was explained by the degree of heterogeneity. The results presented here in Figure 2, however, show fractal scaling for *Pe* values up to 75,000, many orders of magnitude larger than previous studies. This is a confirmation of previous results that an undulating topography, which is directly accounted for in the current work, plays a significant role in the apparent macrodispersion of residence times of parcels of water in the subsurface [e.g., *Worman et al.*, 2007]. This study demonstrates that the influence of topography persists also under transient conditions.

167 In previous scaling analysis, vadose zone or root zone processes have not been
168 considered. Some tracers such as chloride, used in the work of *Kirchner et al.*, [2000], as
169 opposed to isotopic tracers, do not re-equilibrate when exposed to the atmosphere. Chloride
170 residence times will then reflect the time history of pathways between the ground surface and
171 water table. Thus, vadose zone processes, previously ignored by other studies, need to be
172 considered in the analysis. Figure 3 shows the power spectra for case LS, where the vadose
173 and root zone are included in the simulations of travel times. Inspection of the spectra for
174 different *Pe* values shows that *m* of the power spectra increases more continuously with
175 increasing heterogeneity than for the case WT. This is also shown in Figure 4. The slopes now
176 range between $1.04<m>1.38$. In case of $Pe=75$, the power law behavior appears to weaken for
177 larger time scales and approaches a more exponential behavior.
178 Juxtaposition of Figure 2 and 3 show directly the influence of the vadose zone on the
179 residence time distribution spectra for varying degrees of macrodispersion. This is
180 summarized in Figure 4. The vadose zone generally increases the slope of the power spectra,
181 and thus introduces longer range correlations, which can be explained by differences in the
182 variances in the residence time distributions. Processes in the vadose zone also introduce more
183 noise in the power spectra (as shown in Figure 3). This might be because particles become
184 "locked" in the vadose zone through continuous redistribution due to evapotranspiration and
185 infiltration. Vadose and root zone processes may, in a sense, introduce additional stagnation
186 points, similar to those found in the classical Toth problem analysis, and introduction of
187 macrodispersion may smooth the effects of those stagnation points on the power spectra of the
188 age distribution. These stagnation points appear to be important in explaining the scaling
189 behavior of a watershed, however, as large dispersivities appear to destroy this structure to an
190 extent not observed in physical systems.
191 It has been shown previously, that the slope of the power spectra is a measure of
192 stationarity of the data [*Davis et al.*, 1994], where stationarity means that the statistics of the

193 data do not depend on translation along the independent coordinate. For stationary cases, *m* is
194 generally smaller than one and for nonstationary cases, *m* is generally larger than 1. Thus, in
195 the simulations presented here, for *Pe*>7500 and in absence of a vadose zone,
196 macrodispersion appears to increase stationarity and the residence time distributions approach
197 white noise to '1/*f*' noise [*Davis et al.*, 1994]. On the other hand, in case LS, the
198 macrodispersion in conjunction with processes of the vadose zone have the opposite effect.
199 The slope of the power spectrum is larger than one and increases with increasing
200 macrodispersion, which suggests nonstationarity. Thus, the vadose zone being a relatively thin
201 interface has a significant influence on residence time distributions, because of the non-
202 linearity of variably saturated flow and evapotranspiration, which depends on the moisture
203 state of the shallow subsurface.
204
205 **Summary**
206 Using a fully-coupled, groundwater, vadose zone and land surface model in conjunction with
207 a Lagrangian particle tracking model a series of residence time distributions were developed
208 for recharge from the land surface and water table to the riverbed. A spectral analysis of these
209 residence times demonstrated power spectra that exhibit power-law or fractal type behavior
210 previously observed in experimental studies for a wide range of *Pe* numbers. In age
211 distribution cases where the effects of vadose zone processes were not considered, increasing
212 macrodispersion first increases, then decreases the slope of the log-log power spectra below
213 one. In contrast, consideration of vadose and root zone processes on residence time
214 distributions leads to increasing slopes of the log-log power spectra with increasing
215 macrodispersion and slopes always greater than one. Thus, the vadose zone interface of the
216 shallow subsurface has a profound influence on the scaling behavior of the residence time
217 distribution. Following the notion of the slope of the power spectra, *m,* being a measure of
218 stationarity, the vadose zone decreases stationarity of the residence time distribution. That

fractal scaling is demonstrated for much larger *Pe* numbers than in previous studies confirms the importance of topographic also under transient conditions. However, the presented study also shows the influence of land surface and vadose zone processes on the apparent macrodispersion of solutes in groundwater. This indicates that the observed fractal scaling behavior in watersheds might be explained through a combination of these physical processes.

The presented study provides a picture of overall fractal scaling of solutes in watersheds in an integrated fashion i.e. combining various aspects such as topography, macrodispersion, the vadose zone, and land surface processes that have been discussed separately in the literature. The results also suggest that the simulation platform is useful in analyzing path and residence time distributions in real-world system by appropriately capturing the variances over a large range of scales.

Acknowlegements

This work performed under the auspices of the U.S. Department of Energy by Lawrence Livermore National Laboratory under Contract DE-AC52-07NA27344.

References

Ashby, S. F., and R. D. Falgout (1996), A parallel multigrid preconditioned conjugate gradient algorithm for groundwater flow simulations, *Nucl Sci Eng*, *124*(1), 145-159.

Cardenas, M. B. (2007), Potential contribution of topography-driven regional groundwater flow to fractal stream chemistry: Residence time distribution analysis of Toth flow, *Geophys Res Lett*, *34*(5), -.

Dai, Y. J., et al. (2003), The Common Land Model, *B Am Meteorol Soc*, *84*(8), 1013-1023.

Davis, A., et al. (1994), Multifractal Characterizations of Nonstationarity and Intermittency in Geophysical Fields - Observed, Retrieved, or Simulated, *J Geophys Res-Atmos*, *99*(D4), 8055-8072.

Haggerty, R., et al. (2000), On the late-time behavior of tracer test breakthrough curves, *Water Resour Res*, *36*(12), 3467-3479.

Haggerty, R., et al. (2002), Power-law residence time distribution in the hyporheic zone of a 2nd-order mountain stream, *Geophys Res Lett*, *29*(13), -.

Jones, J. E., and C. S. Woodward (2001), Newton-Krylov-multigrid solvers for large-scale, highly heterogeneous, variably saturated flow problems, *Adv Water Resour*, *24*(7), 763-774.

Kirchner, J. W., et al. (2000), Fractal stream chemistry and its implications for contaminant transport in catchments, *Nature*, *403*(6769), 524-527.

Kirchner, J. W., et al. (2001), Catchment-scale advection and dispersion as a mechanism for fractal scaling in stream tracer concentrations, *J Hydrol*, *254*(1-4), 82-101.
Kollet, S. J., and R. M. Maxwell (2006), Integrated surface-groundwater flow modeling: A free-surface overland flow boundary condition in a parallel groundwater flow model, *Adv Water Resour*, *29*(7), 945-958.
Kollet, S. J., and R. M. Maxwell (2007), Capturing the influence of groundwater dynamics on land surface processes using an integrated, distributed watershed model, *Water Resour Res*, (accepted).
LaBolle, E. M., et al. (1996), Random-walk simulation of transport in heterogeneous porous media: Local mass-conservation problem and implementation methods, *Water Resour Res*, *32*(3), 583-593.
LaBolle, E. M., et al. (2006), Diffusive fractionation of H-3 and He-3 in groundwater and its impact on groundwater age estimates, *Water Resour Res*, *42*(7), -.
Lomb, N. R. (1976), Least-Squares Frequency-Analysis of Unequally Spaced Data, *Astrophys Space Sci*, *39*(2), 447-462.
Maxwell, R. M., and W. E. Kastenberg (1999), Stochastic environmental risk analysis: an integrated methodology for predicting cancer risk from contaminated groundwater, *Stoch Env Res Risk A*, *13*(1-2), 27-47.
Maxwell, R. M., et al. (2003), Streamline-based simulation of virus transport resulting from long term artificial recharge in a heterogeneous aquifer, *Adv Water Resour*, *26*(10), 1075-1096.
Maxwell, R. M., and N. L. Miller (2005), Development of a coupled land surface and groundwater model, *J Hydrometeorol*, *6*(3), 233-247.
Maxwell, R. M., and A. F. B. Tompson (2006), SLIM-FAST: A User's Manual, *Lawrence Livermore National Laboratory, Livermore, CA,*, *UCRL-SM-225092*.
Maxwell, R. M., et al. (2007), Revisiting the cape cod bacteria injection experiment using a stochastic modeling approach, *Environ Sci Technol*, *41*(15), 5548-5558.
Press, W. H., et al. (1996), Numerical Recipes in FORTRAN: The Art of Scientific Computing 2nd Ed., *Cambridge University Press*, 963p.
Reed, P. M., et al. (2006), Bridging river basin scales and processes to assess human-climate impacts and the terrestrial hydrologic system, *Water Resour Res*, *42*(7), -.
Scanlon, T. M., et al. (2007), Positive feedbacks promote power-law clustering of Kalahari vegetation, *Nature*, *449*(7159), 209-U204.
Scargle, J. D. (1982), Studies in Astronomical Time-Series Analysis .2. Statistical Aspects of Spectral-Analysis of Unevenly Spaced Data, *Astrophys J*, *263*(2), 835-853.
Tompson, A. F. B., and L. W. Gelhar (1990), Numerical-Simulation of Solute Transport in 3-Dimensional, Randomly Heterogeneous Porous-Media, *Water Resour Res*, *26*(10), 2541-2562.
Tompson, A. F. B., et al. (1998), Analysis of subsurface contaminant migration and remediation using high performance computing, *Adv Water Resour*, *22*(3), 203-221.
Tompson, A. F. B., et al. (1999), Analysis of groundwater migration from artificial recharge in a large urban aquifer: A simulation perspective, *Water Resour Res*, *35*(10), 2981-2998.
Toth, J. (1963), A Theoretical Analysis of Groundwater Flow in Small Drainage Basins, *J Geophys Res*, *68*(16), 4795-&.
Worman, A., et al. (2007), Fractal topography and subsurface water flows from fluvial bedforms to the continental shield, *Geophys Res Lett*, *34*(7), -.

Figure Captions

Figure 1. Three dimensional plot of backwards in time streamlines for the Little Washita watershed. Particle ages are depicted along each pathline in years. The watershed outline is plotted as the solid black line. The time scale is in years of traveltime.

Figure 2. Logarithmic plot of spectral power as a function of wavelength for different values of dispersivity (noted by the Peclet number in each figure) for simulations ending at the water table (case WT). Note that raw spectra are shown in gray, smoothed spectra in black and a linear fit of the spectra shown with the dashed line with the slope (m) given for each case.

Figure 3. Logarithmic plot of spectral power as a function of wavelength for four different values of dispersivity (noted by the Peclet number in each figure) for simulations ending at the ground surface, thus, including vadose zone processes (case LS). Note that raw spectra are shown in gray, smoothed spectra in black and a linear fit of the spectra shown with the dashed line with the slope (m) given for each case.

Figure 4. Semi-logarithmic plot of the slope (m) of a best linear fit to the power spectra as a function of Peclet number for vadose (case LS, triangles) and non-vadose zone (case WT, squares) cases.

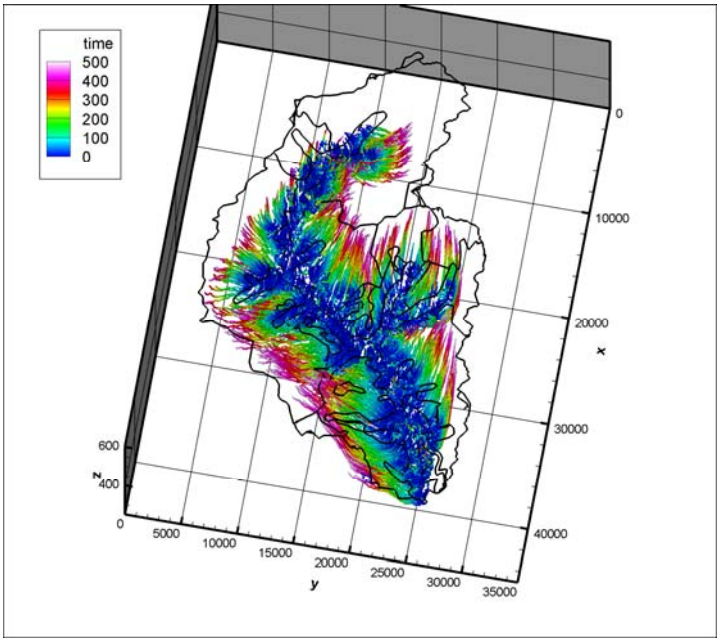
time
500
400
300
200
100
0
z
600
400
0
5000
10000
15000
20000
25000
30000
35000
y
0
10000
20000
30000
40000
x

Figure 1.

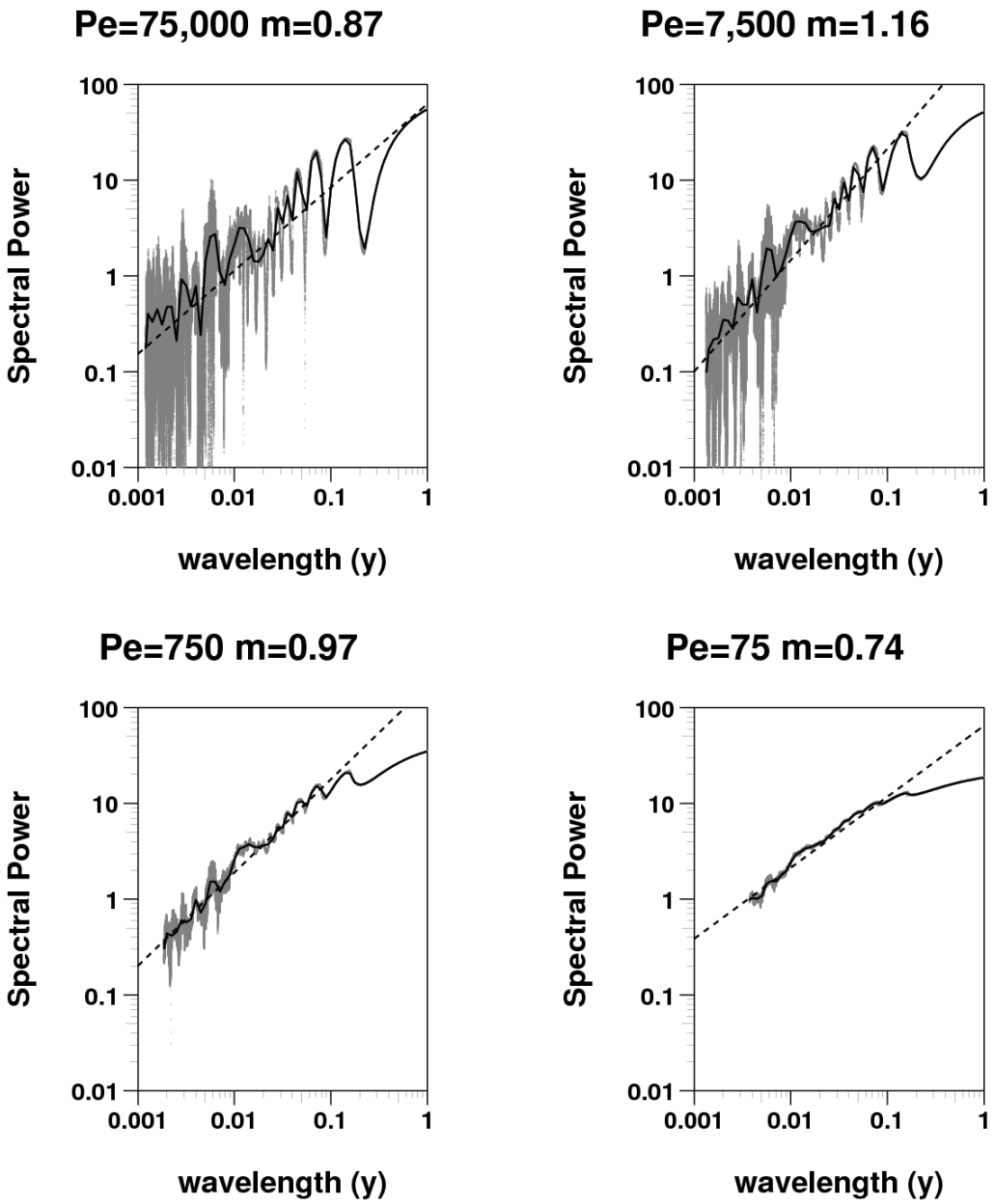

322

323

324 Figure 2.

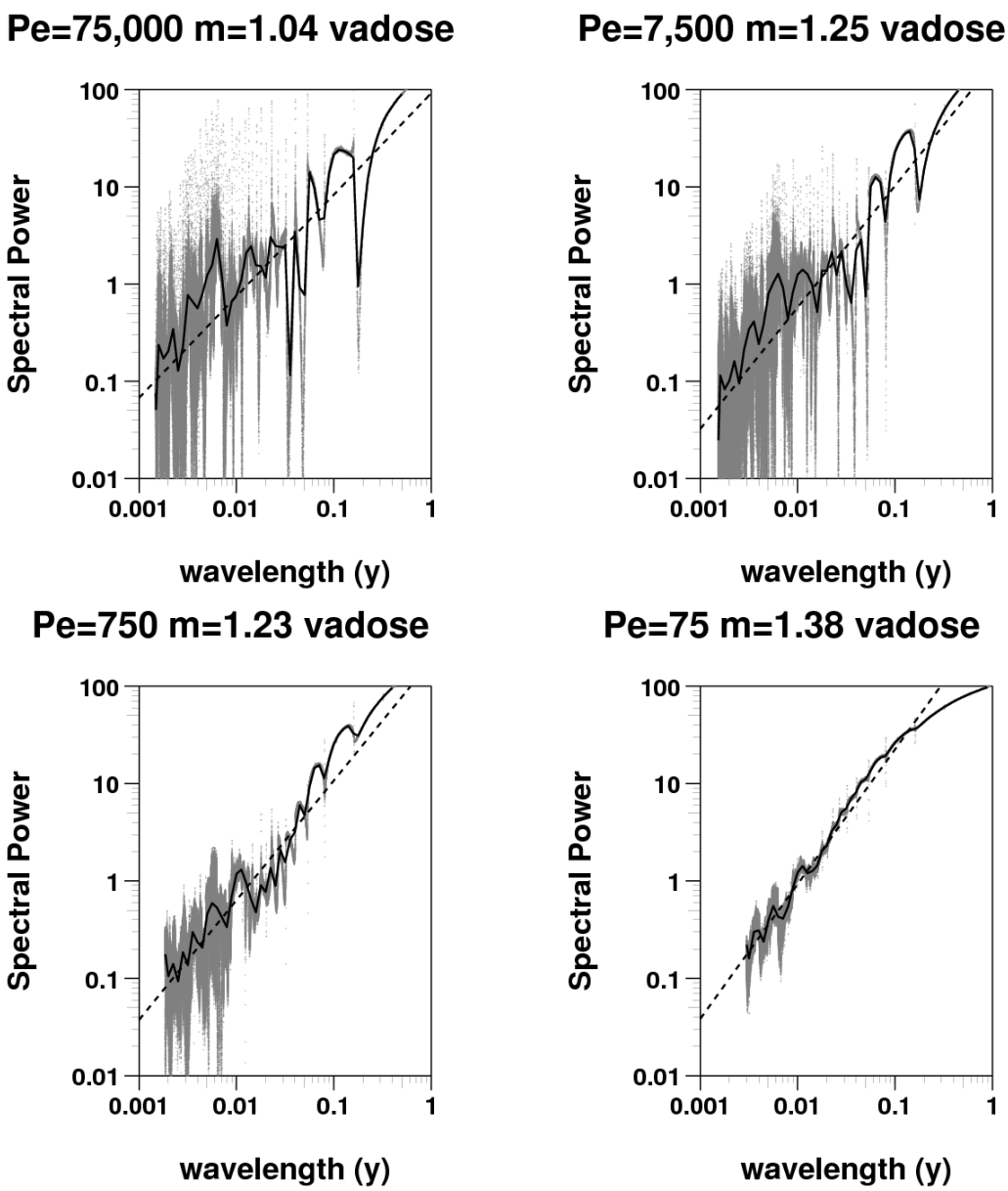

325

326

327 Figure 3.

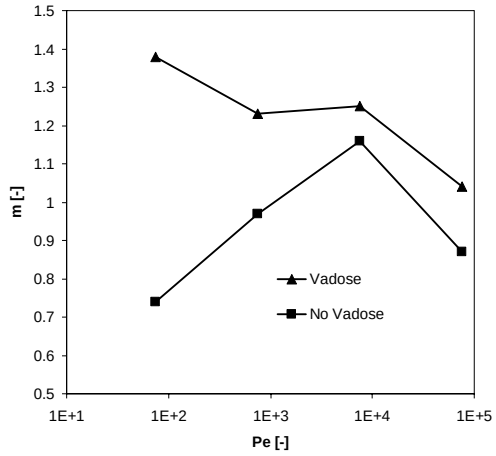

328

329 Figure 4.